Available online at www.sciencedirect.com
ScienceDirect
Journal of Solid State Chemistry 179 (2006) 3214–3223
JOURNAL OF SOLID STATE CHEMISTRY
www.elsevier.com/locate/jssc

Solid-state structural properties of 2,4,6-trimethoxybenzene derivatives, determined directly from powder X-ray diffraction data in conjunction with other techniques

Zhigang Pan[a], Mingcan Xu[a], Eugene Y. Cheung[a], James A. Platts[a], Kenneth D.M. Harris[a,*], Edwin C. Constable[b], Catherine E. Housecroft[b]

[a]*School of Chemistry, Cardiff University, Park Place, Cardiff CF10 3AT, Wales, UK*
[b]*Department of Chemistry, University of Basel, Spitalstrasse 51, 4056 Basel, Switzerland*

Received 1 April 2006; received in revised form 11 May 2006; accepted 11 June 2006
Available online 14 June 2006

Abstract

Structural properties of 2,4,6-trimethoxybenzaldehyde, 2,4,6-trimethoxybenzyl alcohol and 2,4,6-trimethoxyacetophenone have been determined directly from powder X-ray diffraction data, using the direct-space Genetic Algorithm (GA) technique for structure solution followed by Rietveld refinement. Structural similarities and contrasts within this family of materials are elucidated. The work illustrates the value of utilizing information from other sources, including spectroscopic data and computational techniques, as a means of augmenting the structural knowledge established from the powder X-ray diffraction data.

Keywords: Powder X-ray diffraction; Structure determination; Molecular conformation; Solid state NMR; DFT calculations

1. Introduction

Within the last decade or so, new opportunities have been created for carrying out complete structure determination of organic molecular solids directly from powder diffraction data [1], particularly through the development of the direct-space strategy for structure solution [2]. Such techniques are essential for structure determination of the wide range of materials that cannot be prepared as single crystals of suitable size and/or quality for investigation by single crystal X-ray diffraction techniques. Recent advances in methodology within the field of structure determination from powder X-ray diffraction data are such that organic molecular crystal structures of moderate complexity can now be determined fairly routinely by this approach. Nevertheless, structure determination from powder X-ray diffraction data is not a "black-box" technique, and careful attention is required to ensure the correctness of the structure obtained. In this regard, an important aspect, illustrated in the present paper, is to recognize the advantages of using information derived from other sources, including spectroscopic data and/or computational techniques, in conjunction with the powder X-ray diffraction data as a means of augmenting the structural information determined from the diffraction data.

This paper reports the structure determination of three related organic molecular materials (Fig. 1): 2,4,6-trimethoxybenzaldehyde (denoted **1**), 2,4,6-trimethoxybenzyl alcohol (denoted **2**) and 2,4,6-trimethoxyacetophenone (denoted **3**). In each case, structure determination has been carried out directly from powder X-ray diffraction data using our direct-space Genetic Algorithm (GA) technique [3] for structure solution, followed by Rietveld refinement [4]. Materials **1**–**3** are of interest as part of a wider research effort on dendrimeric materials, as they are precursors for some of the targeted families of dendrimers in this research.

2. Experimental details and methodology

Compound **1** was obtained from Aldrich and re-crystallized from dichloromethane/methanol (1:10). Compound **2**

*Corresponding author. Fax: +44 29 2087 4030.
E-mail address: HarrisKDM@cardiff.ac.uk (K.D.M. Harris).

0022-4596/$ - see front matter © 2006 Elsevier Inc. All rights reserved.
doi:10.1016/j.jssc.2006.06.009

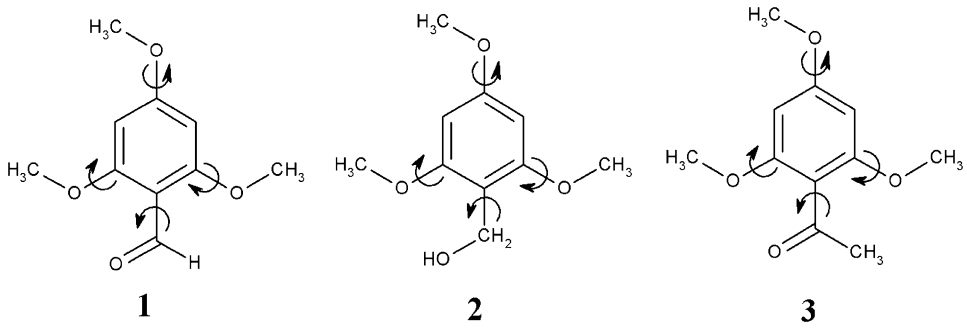

Fig. 1. Molecular structures of **1**, **2** and **3**. The arrows indicate the variable torsion angles in the direct-space structure solution calculations from powder X-ray diffraction data.

was synthesized by reduction of **1** using $LiAlH_4$ in dry THF, purified by column chromatography on silica gel (dichloromethane/methanol, 1:30) and re-crystallized from acetone/hexane (1:4). Characterization of **2** was carried out using standard techniques (solution-state ^1H and ^{13}C NMR and mass spectrometry). To allow solid state ^2H NMR studies to be carried out on **2**, a sample of **2** deuterated in the hydroxyl group (denoted **2**-d) was prepared by refluxing **2** for 24 h in CH_3OD/D_2O (1:5). The suspension was then extracted with dry dichloromethane, dried over sodium sulphate, and evaporated under reduced pressure to afford the crude product, which was re-crystallized from acetone/hexane (1:4). Infrared and NMR spectroscopic experiments on **2**-d indicated that the level of deuteration was ca. 65%. Compound **3** was obtained directly from Aldrich, and used without further purification. For each material, the question of whether the crystal structure contains water or solvent of crystallization was assessed by dissolving an amount of the material in dry $CDCl_3$ and then recording the liquid state ^1H NMR spectrum of the resultant solution. In all cases, there was no evidence for the presence of any water or solvent molecules within the materials **1**–**3** (we note that the same test has been used previously [3d] to assess the presence of water in a crystalline hydrate phase). Furthermore, the solid state ^{13}C NMR spectrum recorded for **1** (see below) is consistent with the conclusion that no solvent (dichloromethane or methanol) molecules are present in the crystal structure.

For measurement of the powder X-ray diffraction patterns of **1**–**3**, the samples were ground using a mortar and pestle and loaded into a borosilicate glass capillary (0.7 mm diameter). Powder X-ray diffraction data were recorded at ambient temperature in transmission mode on a Bruker D8 diffractometer ($CuK\alpha_1$ radiation, Ge-monochromated; VANTEC detector covering 12° in 2θ; total 2θ range 4–70°; step size 0.017°; data collection time 10 h).

Specific details of the structure determination of **1**–**3** from powder X-ray diffraction data are discussed in Section 3. In each case, following indexing (carried out using one or more of the programs ITO [5], TREOR [6] and DICVOL [7]) and pattern decomposition/profile fitting (carried out using the Le Bail technique [8]), structure solution was carried out using a single-population version of the direct-space GA structure solution program EAGER [1g,3,9]. As discussed in Section 3, each of the structures **1**–**3** has one molecule in the asymmetric unit (but different space groups), and in the GA structure solution calculation, each trial structure was defined by a total of 10 variables: $\{x, y, z, \theta, \varphi, \Psi, \tau_1, \tau_2, \tau_3, \tau_4\}$. The four variable torsion angles in each of the molecules **1**–**3** are defined in Fig. 1. In the GA calculation in each case, the population comprised 100 trial structures (with the initial population generated at random). In the evolution of the population from one generation to the next generation, 50 mating operations and 25 mutation operations were carried out. In each case, the correct structure solution was obtained within 20 generations or less. The best trial structure (i.e. the trial structure with lowest R_{wp}) obtained after 20 generations was used as the initial structural model for Rietveld refinement, which was carried out using the GSAS program package [10]. In the Rietveld refinement, standard restraints were applied to bond lengths and bond angles, and planar restraints were applied to the phenyl rings. The restraints on bond lengths and bond angles were relaxed gradually as the refinements progressed. Isotropic displacement parameters were refined for the non-hydrogen atoms. Hydrogen atoms were placed at calculated positions with a fixed value (0.05 $Å^2$) for the isotropic displacement parameter. As discussed elsewhere [3d,4c,4d], careful consideration of the quality of fit achieved in the Rietveld refinement is a crucial component of the validation of the final structural information reported.

Solid state NMR spectra were recorded for powder samples of **1** (^{13}C NMR) and **2**-d (^2H NMR) on a Chemagnetics CMX-Infinity 300 spectrometer (75.48 MHz for ^{13}C; 46.08 MHz for ^2H). The high-resolution solid state ^{13}C NMR spectrum of **1** was recorded under conditions of $^{13}C \leftarrow {}^1H$ cross-polarization (CP), magic angle sample spinning (MAS), high power ^1H decoupling using the TPPM decoupling technique, and total suppression of spinning sidebands (TOSS) (CP contact time, 10 ms; recycle delay, 30 s; MAS frequency, 4 kHz). The broad-line ^2H NMR spectrum of **2**-d (for a non-spinning sample) was recorded using the standard quadrupole echo pulse sequence at several temperatures between 223 and 293 K (^2H 90° pulse length, 2 μs; recycle delay, 6–30 s depending on temperature).

Density functional theory (DFT) calculations were carried out on isolated molecules of **1** and **3** to assess the preferred conformation of the formyl group in **1** and the acetyl group in **3**, using the Gaussian03 package [11]. In terms of the orientations of the O–CH_3 bonds of the three methoxy groups, the conformational properties were taken to be the same as those observed in the crystal structures of **1** and **3** (see below). Starting from these conformations, full geometry optimization was carried out at the HF/6-31*G*(*d*) level [12] (note that there is no significant change in the orientations of the O–CH_3 bonds of the three methoxy groups upon geometry optimization). Energy minima and transition states were located using approximate coordinates from initial scans, again at the HF/6-31*G*(*d*) level, of the potential energy surface for reorientation of the formyl group around the C–CHO bond in the case of **1** and reorientation of the acetyl group around the C–$COCH_3$ bond in the case of **3**. Assignments of energy minima and transition states were confirmed via harmonic frequency calculations. Geometries of the structures corresponding to energy minima and transition states were re-calculated at the more accurate B3LYP/6-31 + *G*(*d*,*p*) level [12,13], and only energy values from these calculations are quoted below.

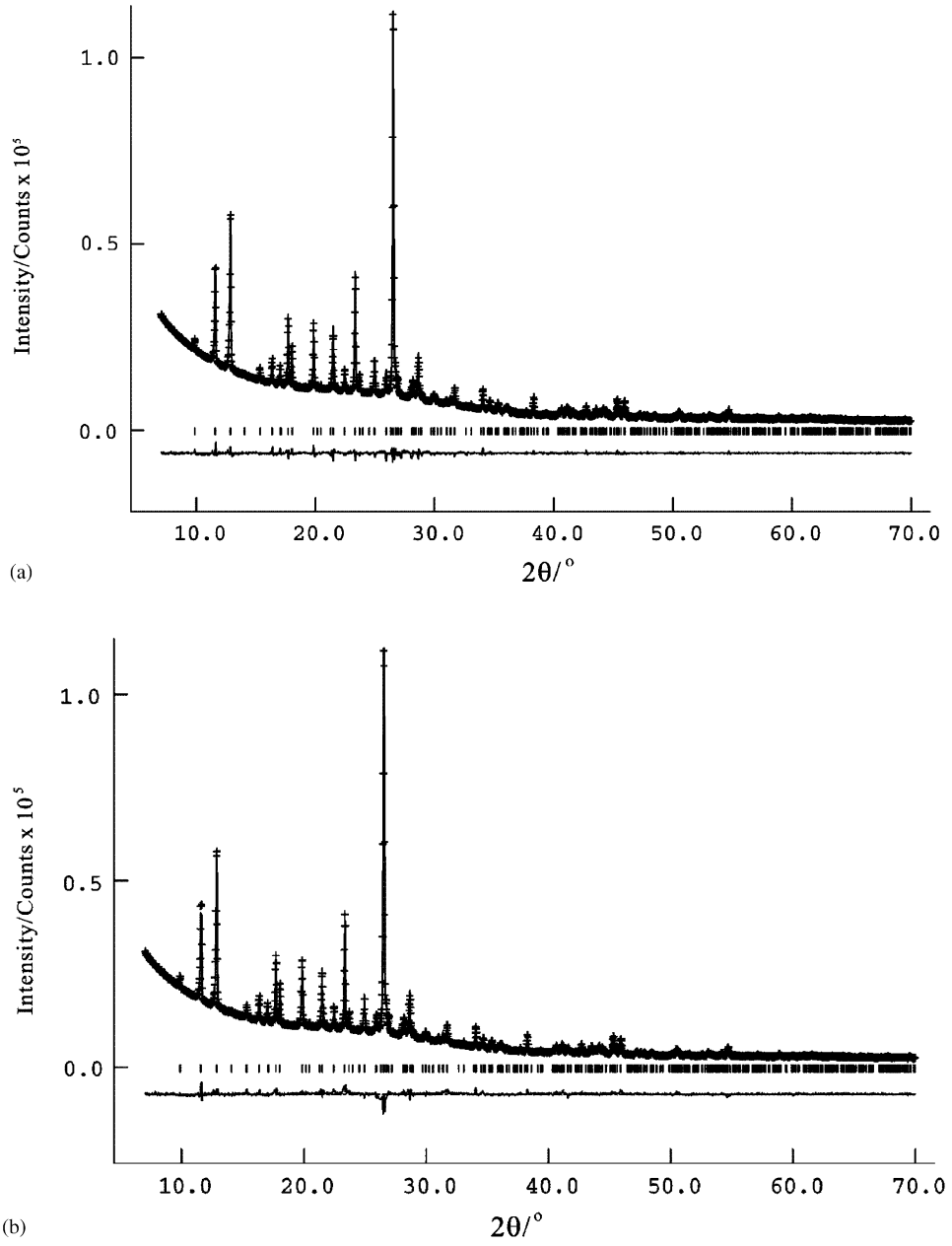

Fig. 2. (a) Le Bail fit and (b) final Rietveld refinement for **1**. The experimental powder X-ray diffraction pattern (+ marks), calculated powder X-ray diffraction pattern (solid line) and difference between experimental and calculated powder X-ray diffraction patterns (lower line) are shown. Tick marks indicate reflection positions.

3. Structure determination from powder X-ray diffraction data

The powder X-ray diffraction pattern of **1** was indexed using the programs ITO ($M_{20} = 213$) and TREOR ($M_{20} = 175$), giving the following unit cell with triclinic metric symmetry: $a = 7.69$ Å, $b = 9.08$ Å, $c = 6.91$ Å, $\alpha = 96.89°$, $\beta = 93.25°$, $\gamma = 81.14°$ ($V = 473$ Å^3). A good quality Le Bail fit (Fig. 2a; $R_{wp} = 2.48\%$, $R_p = 1.54\%$) was obtained using this unit cell, serving both to confirm the correctness of the unit cell and to establish suitable profile parameters for use in the subsequent structure solution calculation. Density considerations suggest that there are two molecules of **1** in the unit cell, and thus the space group is either $P\bar{1}$ with one molecule in the asymmetric unit or $P1$ with two molecules in the asymmetric unit. Structure solution was carried out successfully in space group $P\bar{1}$. In this regard, we note that the high-resolution solid-state ^{13}C NMR spectrum of **1** [14] is consistent with having one independent molecule in the asymmetric unit, in support of our assignment of $P\bar{1}$ as the correct space group (thus the spectrum contains no more than one isotropic peak for each ^{13}C site in the molecule). For completeness, structure solution of **1** was also carried out in space group $P1$, for which there are two molecules in the asymmetric unit (thus, each trial structure was defined by a total of 17 variables—10 variables for one molecule and seven variables for the other molecule, as the positional variables (x, y, z) of one

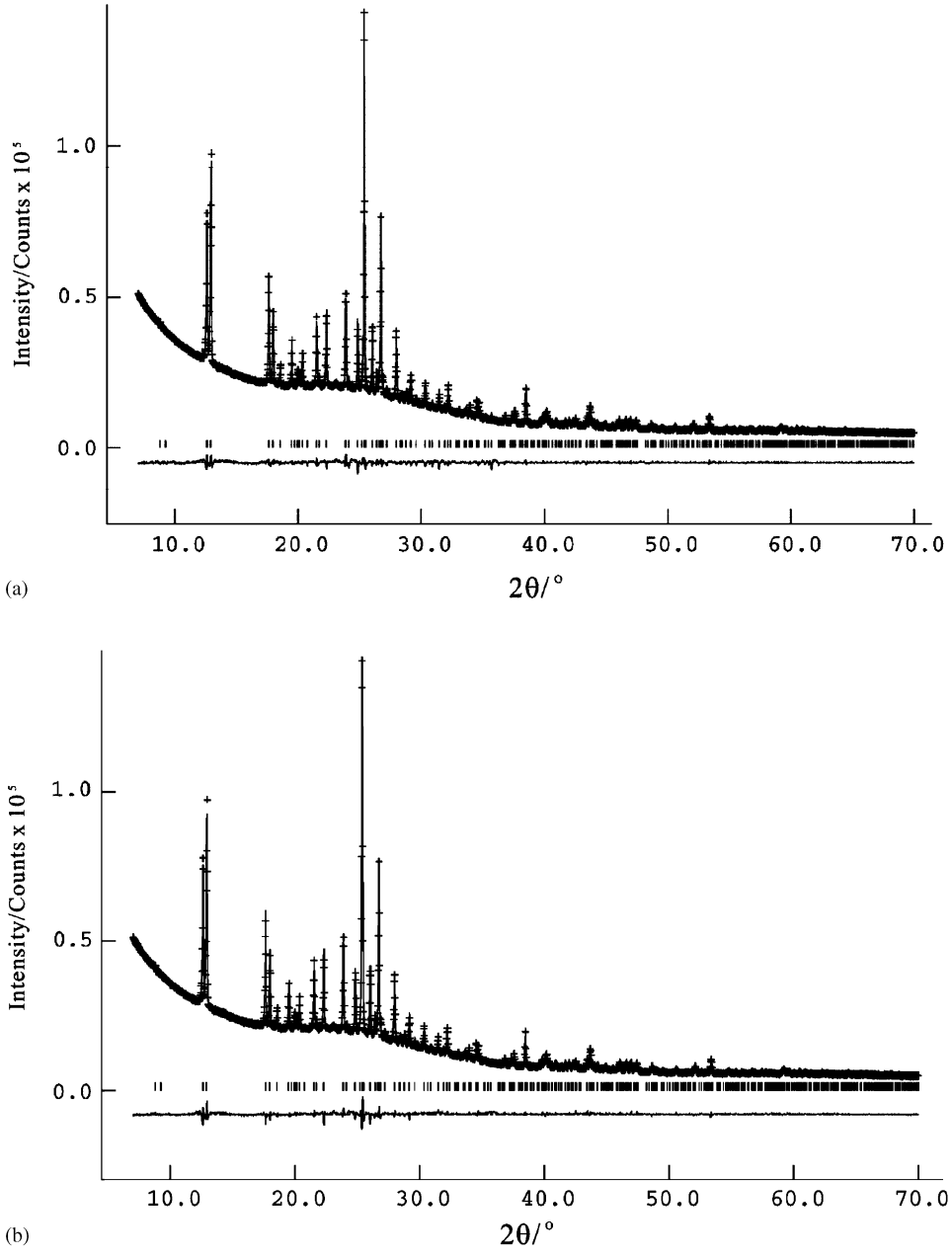

Fig. 3. (a) Le Bail fit and (b) final Rietveld refinement for **2**.

molecule can be fixed arbitrarily in space group $P1$). This calculation also led to a successful structure solution, but the structure was equivalent to that obtained for $P\bar{1}$, suggesting that, consistent with the other evidence presented above, the correct choice of space group is $P\bar{1}$. Following structure solution, Rietveld refinement (in space group $P\bar{1}$) led to a good quality of fit (Fig. 2b; $R_{wp} = 3.56\%$, $R_p = 2.56\%$, $\chi^2 = 11.71$, $R_{F^2} = 0.202$; 3884 profile points, 824 reflections, 43 refined variables), with final refined unit cell parameters: $a = 6.9072(1)$ Å, $b = 7.6947(1)$ Å, $c = 9.0795(2)$ Å, $\alpha = 81.149(2)^\circ$, $\beta = 83.116(1)^\circ$, $\gamma = 86.746(2)^\circ$. We note that the discrepancies between experimental and calculated powder X-ray diffraction patterns in the Rietveld refinement (see the difference plot in Fig. 2b) are comparable to those obtained in the Le Bail fit (see Fig. 2a), thus providing additional vindication that the refinement has been completed successfully. Full details relating to the final refined structure (including fractional coordinates for non-hydrogen atoms) are given as Supporting Information.

The powder X-ray diffraction pattern of **2** was indexed using the program DICVOL ($M_{20} = 33$), giving the following unit cell with monoclinic metric symmetry: $a = 19.12$ Å, $b = 5.10$ Å, $c = 10.05$ Å, $\beta = 91.46^\circ$ ($V = 981$ Å^3). A good quality Le Bail fit (Fig. 3a; $R_{wp} = 2.09\%$, $R_p = 1.40\%$) was obtained for this unit cell and space group, and systematic absences were consistent with space group $P2_1/a$. Density considerations suggest that there are four molecules of **2** in the unit cell, and therefore one molecule in the asymmetric unit. Following successful structure solution, Rietveld

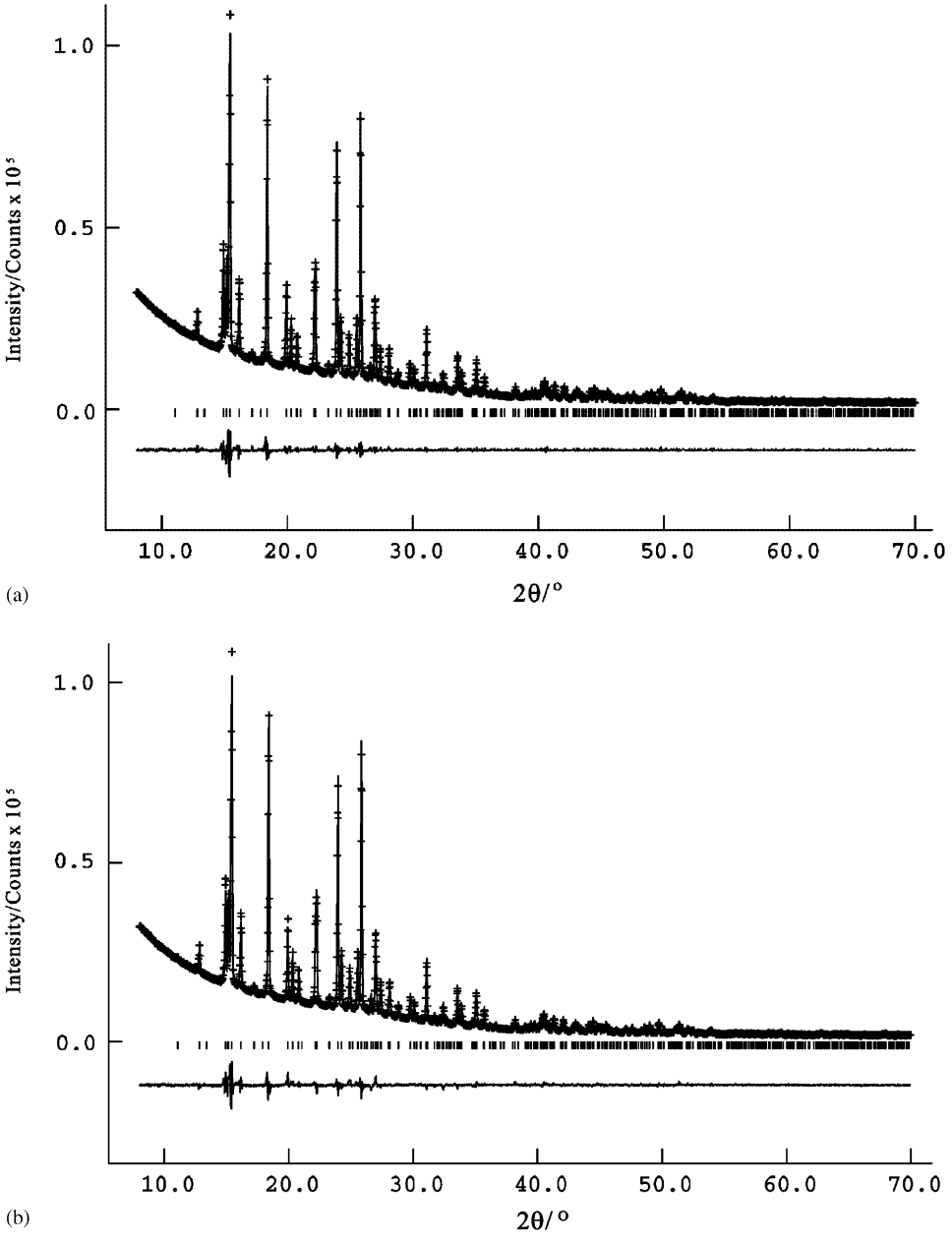

Fig. 4. (a) Le Bail fit and (b) final Rietveld refinement for **3**.

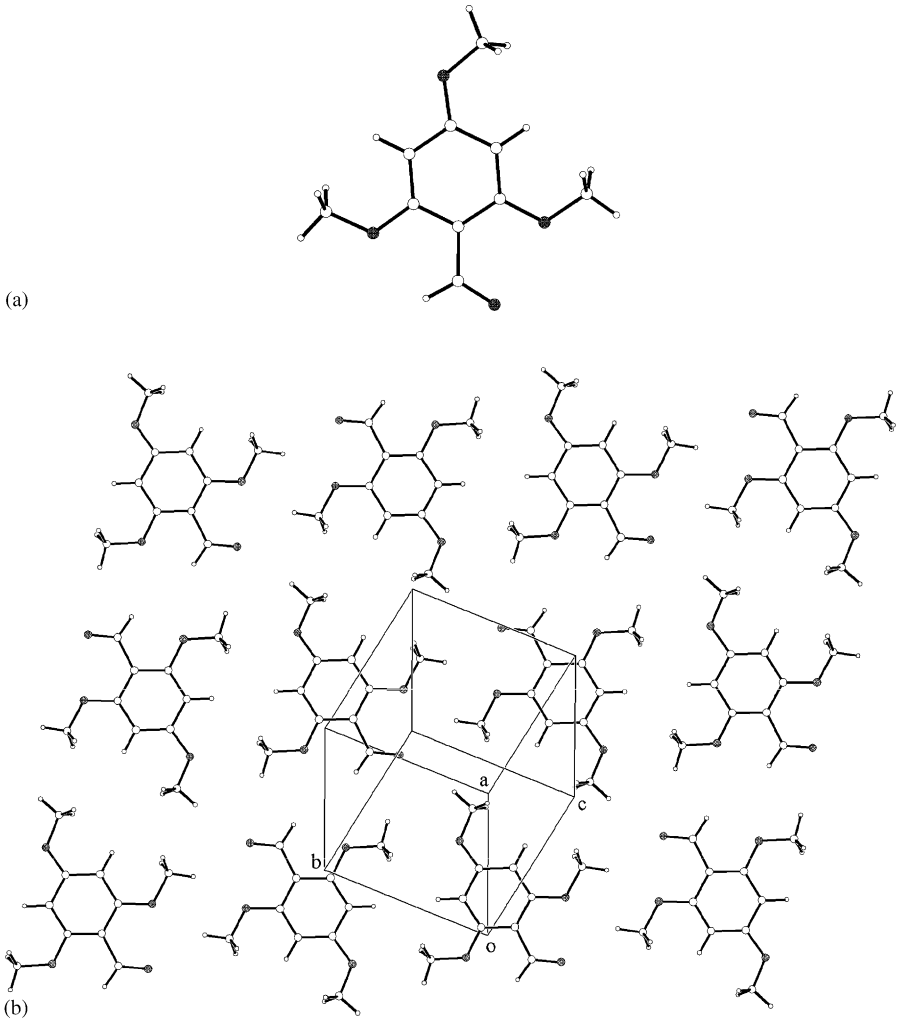

Fig. 5. (a) The molecular conformation in the crystal structure of **1** and (b) the crystal structure of **1** viewed perpendicular to the layers in the structure.

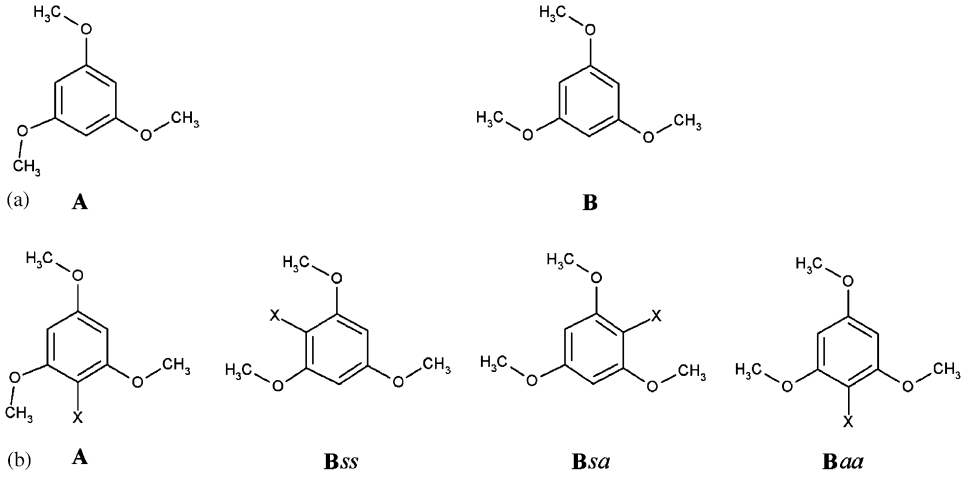

Fig. 6. Conformational possibilities for: (a) a 2,4,6-trimethoxy-substituted benzene ring with the methoxy substituents lying in the plane of the ring, and (b) a 2,4,6-trimethoxy-substituted benzene ring with a substituent (X) in the 1-position and the methoxy-substituents lying in the plane of the ring.

refinement led to a good quality of fit (Fig. 3b; $R_{wp} = 2.72\%$, $R_p = 1.96\%$, $\chi^2 = 13.08$, $R_{F^2} = 0.190$; 3884 profile points, 862 reflections, 43 refined variables), with discrepancies between experimental and calculated powder X-ray diffraction patterns that are comparable to those obtained in the Le Bail fit (Fig. 3a). The unit cell parameters obtained in the final refinement are: $a = 19.1211(3)$ Å, $b = 5.1010(1)$ Å, $c = 10.0497(1)$ Å, $\beta = 91.454(1)^\circ$. Full

details relating to the final refined structure (including fractional coordinates) are given as Supporting Information.

The powder X-ray diffraction pattern of **3** was indexed using the programs ITO ($M_{20} = 42$) and DICVOL ($M_{20} = 43$), giving the following unit cell with monoclinic metric symmetry: $a = 13.59$ Å, $b = 11.67$ Å, $c = 8.55$ Å, $\beta = 126.25°$ ($V = 1093$ Å^3). A good quality Le Bail fit (Fig. 4a; $R_{wp} = 3.18\%$, $R_p = 2.01\%$) was obtained using this unit cell, and systematic absences were consistent with space group $P2_1/a$. Density considerations suggest that there are four molecules of **3** in the unit cell, and thus one molecule in the asymmetric unit. Following successful structure solution, Rietveld refinement led to a good quality of fit (Fig. 4b; $R_{wp} = 3.75\%$, $R_p = 2.46\%$, $\chi^2 = 15.53$, $R_{F^2} = 0.124$; 3884 profile points, 960 reflections, 46 refined variables), with discrepancies between experimental and calculated powder X-ray diffraction patterns that are comparable to those obtained in the Le Bail fit (Fig. 4a). The unit cell parameters obtained in the final refinement are: $a = 13.5783(2)$ Å, $b = 11.6624(2)$ Å, $c = 8.5413(1)$ Å, $\beta = 126.266(1)°$. Full details relating to the final refined structure (including fractional coordinates) are given as Supporting Information.

4. Results and discussion

The molecular conformation in the crystal structure of **1** is shown in Fig. 5a. The three O–CH_3 bonds lie close to the plane of the phenyl ring. For a 2,4,6-trimethoxy-substituted benzene ring in which the methoxy substituents lie in the plane of the ring, there are two possible conformations (denoted **A** and **B**), as shown in Fig. 6. In conformation **A**, each pair of methoxy substituents has a *syn,anti* relationship (where the designations *syn* and *anti* refer to the orientations of the O–CH_3 bonds relative to the orientation of the C(ring)–H bond that lies between the two O–CH_3 substituents). For conformation **B**, on the other hand, one pair of methoxy substituents has a *syn,syn* relationship, one pair has a *syn,anti* relationship and one pair has an *anti,anti* relationship. We now consider replacing one of the C(ring)–H bonds by a C(ring)–X bond (in which the conformation of the X substituent is not specified at this stage), as shown in Fig. 6. For the three methoxy substituents in conformation **A**, replacement of any of the C(ring)–H bonds leads to an identical conformation. For the three methoxy substituents in conformation **B**, on the other hand, the resulting molecular conformation is different depending on whether the substituent X is positioned between the *syn,syn* pair of methoxy substituents, the *syn,anti* pair or the *anti,anti* pair. As shown in Fig. 6, this leads to three different conformations, denoted **B***ss*, **B***sa* and **B***aa*. Thus, in total, there are four possible conformational states for a 2,4,6-trimethoxy-substituted benzene ring with a substituent (X) in the 1-position and the methoxy substituents lying in the plane of the ring. Clearly, from Fig. 5a, the molecular conformation of **1** in the crystal structure corresponds to conformation **B***aa*. Indeed, this conformation is commonly observed in the crystal structures of other molecules containing 2,4,6-trimethoxyphenyl rings [15] (see also the discussion below).

We now consider the conformational properties of the formyl group in the crystal structure of **1**. As shown in Fig. 5b, the plane of the formyl group lies close to the plane of the phenyl ring, and thus there is a relatively short intramolecular O···O contact to the oxygen atom of a methoxy group. Our DFT calculations concur that the observed conformation is the lowest energy conformation with regard to reorientation of the formyl group about the C(1)–CHO bond for the isolated molecule of **1** (with the conformation of the remainder of the molecule, particularly concerning the methoxy groups, taken to be the same as in the crystal structure). As shown in Fig. 7, reorientation of the formyl group gives rise to two energy minima (both with C_s symmetry), corresponding to *syn* and *anti* arrangements of the C=O bond of the formyl group and the O–CH_3 bond of the methoxy group in the 4-position. The former (i.e. *syn*) minimum is lower in energy by 0.79 kJ mol^{-1}, and corresponds to the conformation observed in the crystal structure. A transition structure linking these minima is located when the C–C(1)–C=O torsion angle is ca. 90.9° (i.e. with the plane of the formyl group nearly perpendicular to the plane of the aromatic ring). This transition state is higher in energy than the lower minimum by 23.6 kJ mol^{-1}, and has a single imaginary frequency of 142.5*i* cm^{-1}. We note that similar conformational properties are observed for the formyl group in the crystal structure of 4-hydroxy-2,6-dimethoxybenzaldehyde [16], which is again flanked by two methoxy groups in an *anti,anti* conformation, and the plane of the formyl group lies close to the plane of the phenyl ring.

In the crystal structure of **1** (Fig. 5b), the molecules are arranged in layers parallel to the (112) plane, and interact through van der Waals interactions within the layer. The

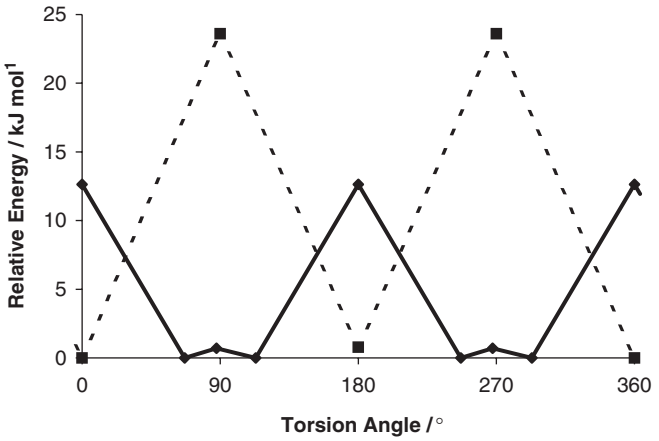

Fig. 7. Results from DFT calculations for the isolated molecules **1** (■) and **3** (◆). The data points represent the results of calculations carried out at the B3LYP/6-31 + *G*(*d*,*p*) level for energy minima and transition states. The straight lines between data points are drawn simply to identify which data points "belong" to a given molecule.

stacking of layers on top of each other is such that there are no $\pi\cdots\pi$ interactions. The oxygen atom of a methoxy group in one layer lies approximately above the centre of the phenyl ring of a molecule in an adjacent layer, and the phenyl rings are offset from each other such that there is no "overlap" of the π systems of molecules in adjacent layers.

The molecular conformation in the crystal structure of **2** is shown in Fig. 8a. The three methoxy groups lie close to the plane of the phenyl ring, and the relative orientations of the O–CH_3 bonds of the methoxy groups correspond to the same conformation (i.e. **B***aa*) observed in the crystal structure of **1**. The oxygen atom of the hydroxyl group lies out of the plane of the phenyl ring. The torsion angle around the C–C bond that links the CH_2OH group to the phenyl ring is ca. 73°. In the crystal structure, the molecules are stacked in columns along the *b*-axis (Fig. 8b and c).

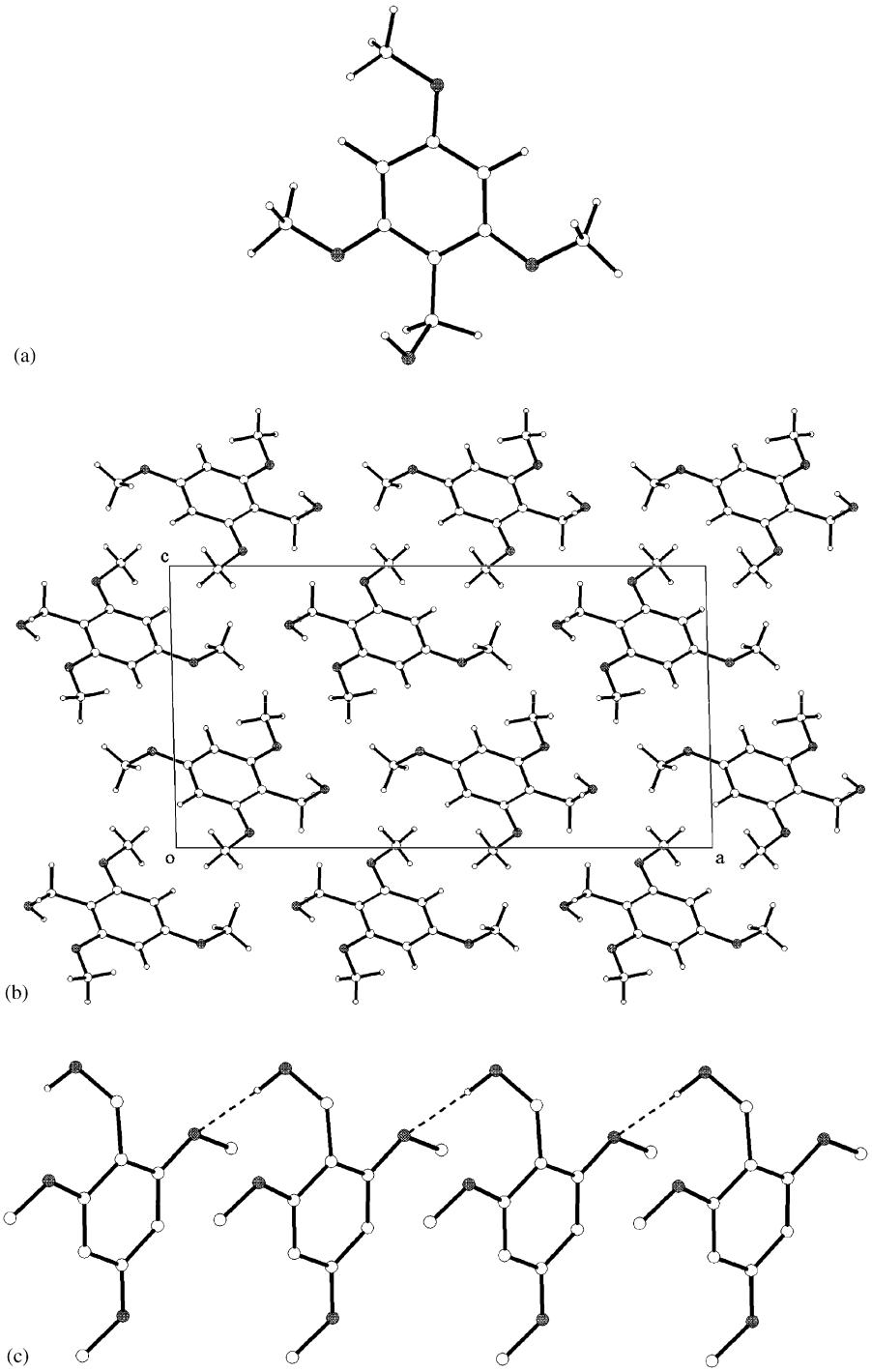

Fig. 8. (a) The molecular conformation in the crystal structure of **2**; (b) the crystal structure of **2** viewed along the *b*-axis; and (c) a hydrogen bonded stack of molecules that runs along the *b*-axis in the crystal structure of **2**.

Adjacent molecules along the stack are related to each other by the unit cell translation (5.10 Å), and are linked by an O–H···O hydrogen bond involving the OH group of one molecule as the hydrogen bond donor and an oxygen atom of a methoxy group of the neighbouring molecule as the hydrogen bond acceptor (Fig. 8c). As the O···O distance for this interaction (3.18 Å) lies towards the upper end of the range for O–H···O hydrogen bonds (although we note that the C–O···O angle, 109.9°, is very close to optimal for a linear O–H···O hydrogen bond), we sought independent assessment of whether the hydroxyl hydrogen atom is indeed engaged in a hydrogen bonding interaction. Thus, ^{2}H NMR studies were carried out on a sample of **2** (denoted **2**-d) deuterated in the hydroxyl group, motivated by the fact that the magnitude of the static ^{2}H NMR quadrupole coupling constant (χ) is known [17] to provide a sensitive probe of whether a deuterated hydroxyl group is involved in O–D···O hydrogen bonding. The static quadrupole interaction parameters measured for **2**-d at 223 K were $\chi = 240$ kHz and η (asymmetry parameter) = 0.075. The observed magnitude of χ lies in the range characteristic of deuterated hydroxyl groups in O–D···O hydrogen bonds, and thus provides independent spectroscopic evidence for the existence of hydrogen bonding in this structure. In the crystal structure, the relatively large tilt angle of the planes of the phenyl rings with respect to the stacking axis is such that there are no significant $\pi\cdots\pi$ stacking interactions between adjacent molecules along the stack. As shown in Fig. 8b (in which the structure is projected on to the plane perpendicular to the *b*-axis), adjacent stacks are in van der Waals contact with each other.

The conformational properties of the methoxy groups in the crystal structure of **3** (Fig. 9a) are similar to those of **1** and **2** in their crystal structures. The three methoxy groups lie close to the plane of the phenyl ring, and the relative orientations of the O–CH_3 bonds of the methoxy groups correspond to the same conformation (i.e. **B***aa*) observed in the crystal structures of **1** and **2**. The torsion angle [C–C(1)–C=O] around the C–C bond that links the acetyl group to the phenyl ring is 66.3°. From the results of our DFT calculations (Fig. 7), it is clear that this conformation of the acetyl group is close to the optimal conformation for the isolated molecule, for which the corresponding torsion angle in the conformation of lowest energy is 66.8°. The conformation with the plane of the acetyl group lying in the same plane as the phenyl ring is a transition state for rotation about the C–$COCH_3$ bond, and is higher than the energy minimum by 12.6 kJ mol^{-1}; the conformation with the plane of the acetyl group perpendicular to the plane of the phenyl ring is also a transition state, and is higher than the lowest energy conformation by 0.71 kJ mol^{-1}. The crystal structure of **3** is shown in Fig. 9b. The phenyl rings of the molecules along the *c*-axis are parallel to each other, but there are no significant $\pi\cdots\pi$ stacking interactions, and the packing of the molecules of **3** in the crystal structure is dominated by van der Waals interactions.

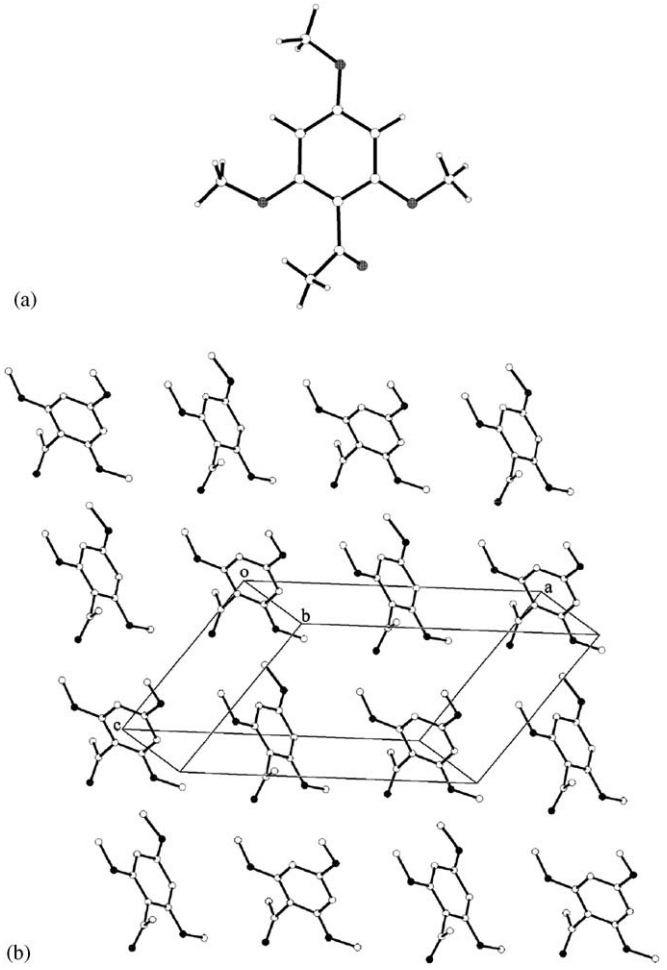

Fig. 9. (a) The molecular conformation in the crystal structure of **3**, and (b) the crystal structure of **3** viewed almost along the *b*-axis.

5. Concluding remarks

The structures of **1**–**3** reported in this paper reveal several interesting insights into structural properties of 2,4,6-trimethoxybenzene derivatives. In each case, the structure was determined straightforwardly from laboratory powder X-ray diffraction data, using the direct-space GA technique for structure solution followed by Rietveld refinement. While the results obtained from the powder X-ray diffraction data in these cases did not yield any structural ambiguities, this work has nevertheless served to illustrate the values of using other sources of information (particularly results from solid-state NMR spectroscopy and DFT calculations) to augment the structural knowledge established from the diffraction data. It is interesting to note that the conformational properties of the formyl group in the crystal structure of **1** and the acetyl group in the crystal structure of **3** are very similar to those in the lowest energy conformational states of the isolated molecules of **1** and **3**, established from our DFT calculations. In these cases, the packing of molecules in the crystal is dominated by van der Waals interactions, and there are no specific interactions involving the formyl and acetyl

groups other than van der Waals interactions. In the crystal structure of **2**, on the other hand, the conformational properties of the hydroxymethyl group are governed by the formation of intermolecular O–H···O hydrogen bonds.

Acknowledgments

We are grateful to EPSRC for general support (to KDMH) and to Bruker AXS and the University of Birmingham for the award of a Ph.D. studentship (to ZP).

Appendix A. Supplementary Materials

Supplementary data associated with this article can be found in the online version at doi:10.1016/j.jssc.2006.06.009.

References

[1] (a) K.D.M. Harris, M. Tremayne, Chem. Mater. 8 (1996) 2554;
(b) K.D.M. Harris, M. Tremayne, B.M. Kariuki, Angew. Chem. Int. Ed. 40 (2001) 1626;
(c) V.V. Chernyshev, Russ. Chem. Bull. 50 (2001) 2273;
(d) W.I.F. David, K. Shankland, L.B. McCusker, C. Baerlocher (Eds.), Structure Determination from Powder Diffraction Data, Oxford University Press/IUCr, 2002;
(e) K.D.M. Harris, E.Y. Cheung, Chem. Soc. Rev. 33 (2004) 526;
(f) A. Altomare, R. Caliandro, M. Camalli, C. Cuocci, C. Giacovazzo, A.G.G. Moliterni, R. Rizzi, R. Spagna, J. Gonzalez-Platas, Z. Kristallogr. 219 (2004) 833;
(g) K.D.M. Harris, S. Habershon, E.Y. Cheung, R.L. Johnston, Z. Kristallogr. 219 (2004) 838;
(h) V. Favre-Nicolin, R. Černý, Z. Kristallogr. 219 (2004) 847;
(i) K. Shankland, A.J. Markvardsen, W.I.F. David, Z. Kristallogr. 219 (2004) 857.
[2] K.D.M. Harris, M. Tremayne, P. Lightfoot, P.G. Bruce, J. Am. Chem. Soc. 116 (1994) 3543.
[3] (a) B.M. Kariuki, H. Serrano-González, R.L. Johnston, K.D.M. Harris, Chem. Phys. Lett. 280 (1997) 189;
(b) K.D.M. Harris, R.L. Johnston, B.M. Kariuki, Acta Crystallogr. Sect. A 54 (1998) 632;
(c) S. Habershon, K.D.M. Harris, R.L. Johnston, J. Comp. Chem. 24 (2003) 1766;
(d) Z. Pan, E.Y. Cheung, K.D.M. Harris, E.C. Constable, C.E. Housecroft, Cryst. Growth Des. 5 (2005) 2084.
[4] (a) H.M. Rietveld, J. Appl. Crystallogr. 2 (1969) 65;
(b) R.A. Young (Ed.), The Rietveld Method, IUCr, Oxford, 1993;
(c) L.B. McCusker, R.B. Von Dreele, D.E. Cox, D. Louër, P. Scardi, J. Appl. Crystallogr. 32 (1999) 36;
(d) L. Eriksson, D. Louër, P.-E. Werner, J. Solid State Chem. 81 (1989) 9.
[5] J.W. Visser, J. Appl. Crystallogr. 2 (1969) 89.
[6] P.-E. Werner, L. Eriksson, M. Westdahl, J. Appl. Crystallogr. 18 (1985) 367.
[7] (a) A. Boultif, D. Louër, J. Appl. Crystallogr. 24 (1991) 987;
(b) A. Boultif, D. Louër, J. Appl. Crystallogr. 37 (2004) 724.
[8] A. Le Bail, H. Duroy, J.L. Fourquet, Mater. Res. Bull. 23 (1988) 447.
[9] S. Habershon, G.W. Turner, Z. Zhou, B.M. Kariuki, E.Y. Cheung, A.J. Hanson, E. Tedesco, D. Albesa-Jové, M.-H. Chao, O.J. Lanning, R.L. Johnston, K.D.M. Harris, EAGER—A Computer Program for Direct-Space Structure Solution from Powder X-ray Diffraction Data, Cardiff University and University of Birmingham.
[10] A.C. Larson, R.B. Von Dreele, GSAS, Los Alamos Laboratory Report No. LA-UR-86-748, 1987.
[11] M.J. Frisch, G.W. Trucks, H.B. Schlegel, G.E. Scuseria, M.A. Robb, J.R. Cheeseman, J.A. Montgomery Jr., T. Vreven, K.N. Kudin, J.C. Burant, J.M. Millam, S.S. Iyengar, J. Tomasi, V. Barone, B. Mennucci, M. Cossi, G. Scalmani, N. Rega, G.A. Petersson, H. Nakatsuji, M. Hada, M. Ehara, K. Toyota, R. Fukuda, J. Hasegawa, M. Ishida, T. Nakajima, Y. Honda, O. Kitao, H. Nakai, M. Klene, X. Li, J.E. Knox, H.P. Hratchian, J.B. Cross, C. Adamo, J. Jaramillo, R. Gomperts, R.E. Stratmann, O. Yazyev, A.J. Austin, R. Cammi, C. Pomelli, J.W. Ochterski, P.Y. Ayala, K. Morokuma, G.A. Voth, P. Salvador, J.J. Dannenberg, V.G. Zakrzewski, S. Dapprich, A.D. Daniels, M.C. Strain, O. Farkas, D.K. Malick, A.D. Rabuck, K. Raghavachari, J.B. Foresman, J.V. Ortiz, Q. Cui, A.G. Baboul, S. Clifford, J. Cioslowski, B.B. Stefanov, G. Liu, A. Liashenko, P. Piskorz, I. Komaromi, R.L. Martin, D.J. Fox, T. Keith, M.A. Al-Laham, C.Y. Peng, A. Nanayakkara, M. Challacombe, P.M.W. Gill, B. Johnson, W. Chen, M.W. Wong, C. Gonzalez, J.A. Pople, Gaussian 03, Revision B.05, Gaussian, Inc., Pittsburgh, PA, 2003.
[12] (a) R. Ditchfield, W.J. Hehre, J.A. Pople, J. Chem. Phys. 54 (1971) 724;
(b) W.J. Hehre, R. Ditchfield, J.A. Pople, J. Chem. Phys. 56 (1972) 2257;
(c) M.S. Gordon, Chem. Phys. Lett. 76 (1980) 163;
(d) P.C. Hariharan, J.A. Pople, Theor. Chim. Acta 28 (1973) 213;
(e) T. Clark, J. Chandrasekhar, G.W. Spitznagel, P.v.R. Schleyer, J. Comput. Chem. 4 (1983) 294.
[13] (a) A.D. Becke, J. Chem. Phys. 98 (1993) 5648;
(b) C. Lee, W. Yang, R.G. Parr, Phys. Rev. B 37 (1988) 785.
[14] In the high-resolution solid state ^{13}C NMR spectrum of **1**, there is a single peak at 185 ppm assigned to the carbonyl carbon. There are two peaks at 55 ppm assigned to the methoxy carbon atoms (with the implication that there is overlap of the three peaks anticipated for a single molecule of **1**), and there are six peaks in the range 80–170 ppm assigned to the aromatic carbons.
[15] (a) C.M.L. van de Velde, L.-J. Chen, J.K. Baeke, M. Moens, P. Dieltiens, H.J. Geise, M. Zeller, A.D. Hunter, F. Blockhuys, Cryst. Growth Des. 4 (2004) 823;
(b) M. Tacke, L.P. Cuffe, W.M. Gallagher, Y. Lou, O. Mendoza, H. Muller-Bunz, F.J.K. Rehmann, N. Sweeney, J. Inorg. Biochem. 98 (2004) 1987;
(c) W. He, X.-F. Sun, A.J. Frontier, J. Am. Chem. Soc. 125 (2003) 14278;
(d) D.H.R. Barton, D.M.X. Donnelly, P.J. Guiry, J.H. Reibenspies, Chem. Commun. (1990) 1110.
[16] C. Wuyts, C.M.L. van de Velde, H.J. Geise, F. Blockhuys, Acta Crystallogr. Sect. E 61 (2005) o79.
[17] (a) G. Soda, T. Chiba, J. Chem. Phys. 50 (1969) 439;
(b) A.E. Aliev, K.D.M. Harris, Struct. Bond. 108 (2004) 1.